



Phosphorus Budget Analysis and Alum Dosage Estimation for Big Chetac Lake, Wisconsin



Big Chetac Lake, 2013

13 December, 2013

*University of Wisconsin – Stout
Discovery Center - Sustainability Sciences Institute
Menomonie, WI 54751
715-338-4395
williamfjames@charter.net
jamesw@uwstout.edu*

SUMMARY

Phosphorus (P) budget analysis of the 2007 summer limnological data set confirmed that internal P loading, primarily from anaerobic sediments located in the north basin, is the dominant P source driving algal blooms in Big Chetac Lake. Empirical steady-state models predicted that management of internal P loading in the north basin would result in a 47% decrease in mean summer total P concentrations to 0.045 mg/L. Predicted chlorophyll concentrations declined by 60% to 21 µg/L and frequency of nuisance algal blooms (i.e., chlorophyll concentrations > 30 µg/L) decreased from 73% to only 19% of the time during the summer. In contrast, management and reduction of tributary P loads resulted in minor predicted improvements in limnological characteristics because these inputs were low relative to P inputs via internal loads.

Sediments in the north basin exhibited very high concentrations of both total P and P fractions that are typically correlated with internal P loading (i.e., loosely-bound and iron-bound P or redox-sensitive P). High concentrations, representing P in excess burial and transformation occurred over the upper 10 to 12 cm sediment layer. Aluminum (Al) sulfate dosage required to inactivate this redox-sensitive P fraction was 135 g/m². It is recommended that a relatively large area in the north basin that included depths greater than 20 ft and an area north of the deepest region be treated with Al. Estimated treatment cost was 1.72 million dollars. Because application of aluminum sulfate temporarily decreases pH, it is recommended that the overall dosage be split into smaller Al applications over a 2 to 3 year period. Thus, one-third or one-half of the total Al dose would be applied in May over consecutive years to prevent pH from declining temporarily below 6.0 (i.e., Al³⁺ solubility increases below this pH and can be toxic to biota).

OBJECTIVES

Summer phosphorus budget analysis of Big Chetac Lake, Wisconsin, indicates that internal phosphorus (P) loading from anaerobic sediments represents a potentially important P flux contribution for algal uptake and growth during the summer (Short Elliott Hendrickson 2009). In order to develop sound and effective alternatives to manage internal P loading in the lake, information is needed on current conditions and predicted future limnological response to a reduction in internal P loading. One management technique often used to successfully reduce anaerobic P release from sediments is application of alum (aluminum sulfate) or buffered alum (aluminum sulfate-sodium aluminate). Alum reacts with lake water to form aluminum hydroxide flocs that settle to the sediment and irreversibly bind P fractions (i.e., primarily porewater P, loosely-bound

P, and iron-bound P) that play an active role in P release from sediment. The objectives of this investigation were several-fold:

1. Explore predicted response of lake summer mean P concentrations, algal bloom magnitude, and the frequency of summer algal blooms to a simulated reduction in internal P loading (i.e., via an aluminum sulfate treatment) using steady-state empirical eutrophication modeling approaches (i.e., Bathtub; Walker 1996),
2. Examine spatial and vertical variations in P fractions that are active and mobile in anaerobic P release from sediment (i.e., redox-sensitive P and labile organic P),
3. Quantify the thickness of the sediment layer potentially active in anaerobic P release,
4. Estimate the dosage of Al (i.e., aluminum sulfate as Al, g/m²) required to bind redox-sensitive P fractions in the active sediment layer, and
5. Provide cost estimates for Al application based on treatment areas in the lake.

APPROACH

Phosphorus budget analysis and steady-state empirical modeling

Lake monitoring and hydrological and phosphorus budget information collected in 2007 (Short Elliott Hendrickson 2009) were used to develop steady-state eutrophication models to predict current and future summer limnological conditions in Big Chetac Lake. During that summer (May to September), inflows from several creeks (Benson Cr., Heron Cr., Knuteson Cr., and Red Cedar Spring) discharging into the lake, precipitation, and changes in lake pool elevation were used to develop a hydrological budget,

$$\Delta \text{ lake volume} = (In_{trib} + In_{precip}) - (Out_{lake} + Out_{evap}) \quad 1)$$

where, Δ lake volume = change in lake volume, In_{trib} = tributary inflow from gauged and unmonitored watersheds, In_{precip} = precipitation over the lake surface, and Out_{evap} = evaporation from the lake surface.

Stations were established in the north, central, and south basin of Chetac Lake for limnological monitoring in 2007 (Fig. 1). In situ profiles of water temperature and dissolved oxygen and water samples were collected near the lake surface and at 1-m intervals from the 2.5-depth to the lake bottom at approximately 2-week intervals between late April and October (Short Elliott Hendrickson 2009). Water samples were analyzed for total P (TP), total nitrogen (TN), and chlorophyll.

For phosphorus budget analysis and steady-state empirical modeling, mean concentrations were estimated for each lake basin on each monitoring date as,

$$C_{Basin} = \sum_{z=0}^n C_z \cdot Volume \quad 2)$$

where C_z = the TP or chlorophyll concentration (mg/L or g/m³) and Volume = the water volume (m³) at depth z (m). Surface areas and layer volumes versus depth were provided by Short, Elliott, Hendrickson, Inc (SEH, Inc; Dave Blumer, personal commu.). The product (kg) for each depth layer was summed over the entire water column (n = maximum depth, m) to estimate the mean concentration weighted over the entire water column in each lake basin (C_{Basin}).

Net internal P loading ($P_{net\ internal\ load}$) was defined as the flux of P from sediment stored in the lake in excess of P sedimentation. $P_{net\ internal\ load}$ was estimated by difference from the equation,

$$\Delta P_{lake\ storage} = (P_{external\ load} - P_{outflow}) \pm P_{net\ internal\ load} \quad 3)$$

where $\Delta P_{\text{lake storage}}$ = the change in lake P mass over a defined summer period, $P_{\text{external load}}$ = the P mass input to the lake from measured tributary loads, and P_{outflow} = the P mass that was discharged from the lake. $P_{\text{lake storage}}$ was calculated from equation 2. Mass estimates were converted to rates ($\text{mg}/\text{m}^2 \text{ d}$) by dividing mass by the area of the lake and defined time period (~ 159 days).

Stratification and the potential for mixing were examined by evaluating variations in stability and mean water column temperature. Schmidt stability (S; $\text{g}\cdot\text{cm}/\text{cm}^2$) was calculated as:

$$S = 1/A \int_0^{z_m} (z - z_g)(\rho_z - \rho_g) dz \quad 4)$$

where A = surface area (m^2), z_m = maximum depth (m), z = depth at stratum z , z_g = depth of the center of mass or ρ_g , and ρ_z = the density of water (kg/m^3) at depth z (Idso 1973). ρ_g was calculated as:

$$\rho_g = 1/V \int_0^{z_m} V_z \rho_z dz \quad 5)$$

where V is lake volume (m^3) and V_z is the volume at depth z . Schmidt stability represented the amount of work (in the form of wind power, motor boat activity, etc) required to completely mix a water body that is stratified due to vertical differences in water density. Higher stability values were indicative of strong stratification and greater work required to disrupt stratification. Conversely, lower stability values were indicative of weak stratification and less work required to disrupt stratification.

The summer anoxic factor (AF, d/summer), days that a sediment area normalized with respect to the lake surface area is anoxic, was quantified for 2007 according to the following equation developed by Nürnberg (1995) as,

$$AF = \frac{\sum_{i=1}^n t_i a_i}{A_{LakeSurface}} \quad 6),$$

where, t_i = the time interval of anoxic conditions (d), a_i = anoxic sediment area over the interval (m^2), and $A_{LakeSurface}$ = the lake surface area (m^2). Anoxia was defined as dissolved oxygen concentration less than or equal to 1.0 mg/L.

Steady-state empirical modeling and loading reduction scenarios were examined using *Bathtub* (Walker 1996). *Bathtub* is a windows-based software program that provides a suite of equations for predicting lake average P, chlorophyll, and Secchi transparency. Response of these variables to decreases in P loading (external and internal) was used to evaluate management alternatives.

Spatial and vertical variations in sediment phosphorus

The objectives of this task were twofold: 1) to quantify vertical variations in mobile P forms in the north basin of the lake for use in estimating the thickness of the sediment layer that needs to be treated with Al and 2) to evaluate spatial variations in mobile P in the upper 0-5 and 5-10 cm sediment layer at additional sites. Typically, the Al floc sinks to between 4 and greater than 10 cm during the first several months after treatment, depending on the density of the sediment. There are currently no models or empirical relationships that can be used to predict the extent of Al sinking. However, vertical profiles in sediment physical characteristics and mobile P can be used as an aid in evaluating the probable thickness of the sediment layer active in diffusive P flux. A sediment core was collected at a station located in the deepest area of the north basin for vertical sectioning purposes (Fig. 1). The core was sectioned at 1-cm intervals over the upper 6 cm, 2-cm intervals between 6 and 10 cm, 2.5-cm intervals between 10 and 15 cm, and 5-cm intervals below the 20-cm depth. Additional cores (3 locations), collected at shallower depths in the lake, were sectioned over the upper 5-cm layer and 5- to 10-cm for analysis of variations in the concentration of sediment mobile P as a function of lake

depth. For instance, shallower lake depths may have lower mobile P concentrations and require less Al. This information will be important in more accurately estimating alum dosage and cost.

Sediment sections were analyzed for the constituents listed in Table 1. Subsamples will be dried at 105 °C to a constant weight and burned at 500 °C for determination of moisture content, sediment density, and organic matter content (Håkanson and Jansson 2002). Phosphorus fractionation was conducted according to Hieltjes and Lijklema (1980), Psenner and Puckso (1988), and Nürnberg (1988) for the determination of ammonium-chloride-extractable P (1 M NH₄Cl; loosely-bound P), bicarbonate-dithionite-extractable P (0.11 M BD; iron-bound P), sodium hydroxide-extractable P (0.1 N NaOH; aluminum-bound P), and hydrochloric acid-extractable P (i.e., calcium-bound P). A subsample of the sodium hydroxide extract was digested with potassium persulfate to determine nonreactive sodium hydroxide-extractable P (Psenner and Puckso 1988). Labile organic P was calculated as the difference between reactive and nonreactive sodium hydroxide-extractable P. Refractory organic P was estimated as the difference between total P and the sum of the other fractions.

The loosely-bound and iron-bound P fractions are readily mobilized at the sediment-water interface as a result of anaerobic conditions that lead to desorption of P from sediment and diffusion into the overlying water column (Mortimer 1971, Boström 1984, Nürnberg 1988). The sum of the loosely-bound and iron-bound P fraction represents redox-sensitive P (i.e., the P fraction that is active in P release under anaerobic and reducing conditions; redox-P). In addition, labile organic P can be converted to soluble P via bacterial mineralization (Jensen and Andersen 1992) or hydrolysis of bacterial polyphosphates to soluble phosphate under anaerobic conditions (Gächter et al. 1988, Gächter and Meyer 1993, Hupfer et al. 1995). The sum of redox-P and labile organic P collectively represent biologically-labile P. This fraction is active in recycling pathways that result in exchanges of phosphate from the sediment to the overlying water column and potential assimilation by algae. In contrast, aluminum-bound, calcium-bound, and

refractory organic P fractions are more chemically inert and subject to burial rather than recycling.

Al dosage determination

Additional sediment collected from the north basin of the lake was subjected to a range of aluminum sulfate (as Al) concentrations to determine the dosage required to inactivate the redox-P fraction. Alum (as aluminum sulfate; $\text{Al}_2(\text{SO}_4)_3 \cdot 18 \text{H}_2\text{O}$) was combined with 0.1 M sodium bicarbonate (NaHCO_3) to a concentration of 0.7 to 1.4 g Al L^{-1} to form an aluminum hydroxide ($\text{Al}(\text{OH})_3$) floc. Aliquots of this solution, diluted to a final volume of 10 mL with distilled water, were added to centrifuge tubes containing the equivalent of 0.025 g dry weight (DW) of fresh sediment to obtain Al concentrations ranging from 0 (i.e., control) to greater than 100 mg Al g^{-1} DW sediment or higher. The assay tubes were shaken for a minimum of 2 hours at 20 °C in a darkened environmental chamber, centrifuged at 500 g to concentrate the sediment, and decanted for redox-P determination.

Al dosage was estimated as the concentration (g/m^2) required to bind at least 90% of the redox-P. The dry mass concentration of redox-P (mg/g^1) was converted to an areal concentration (g/m^2) as,

$$\text{Redox-P (g}\cdot\text{m}^{-2}) = \text{Redox-P (mg}\cdot\text{g}^{-1}) \cdot \rho \text{ (g}\cdot\text{cm}^{-3}) \cdot \theta \cdot h \text{ (m)} \cdot 1000000 \text{ (cm}^3\cdot\text{m}^{-3}) \cdot 0.001 \text{ (g}\cdot\text{mg}^{-1}) \quad (6)$$

where, ρ is sediment bulk density ($\text{g}\cdot\text{cm}^{-3}$), θ is sediment porosity (100 – percent moisture content; dimensionless), and h is sediment thickness (m). The Al concentration (g/m^2) was estimated as,

$$\text{Al (g}\cdot\text{m}^{-2}) = \text{Redox-P (g}\cdot\text{m}^{-2}) \cdot \text{Al:P}_{90\%} \quad (7)$$

where, $\text{Al:P}_{90\%}$ is the binding ratio required to adsorb 90% of the redox- P in the sediment.

The area-based (g/m^2) and volume-based (mg/L) concentration of Al was converted to gallons of aluminum sulfate (or a combination of aluminum sulfate-sodium aluminate for softwater lakes) by considering the sediment treatment area, thickness of the active sediment layer, and volume of the north basin. Treatment area was chosen based on summer stratification and hypolimnetic anoxia patterns. This information was converted to a cost estimate to treat the lake based on generic applicator setup fees and the current cost of alum per gallon.

RESULTS AND DISCUSSION

Limnological dynamics summary and steady-state empirical modeling

Overall, Big Chetac Lake is large and shallow with a long maximum fetch along the south-south-west to north-north-east axis, making it susceptible to mixing (Table 2). The Osgood Index for the lake is only 1.5 (i.e., mean depth, m, divided by the square root of the surface area, km^2). Lakes with values < 6 are more susceptible to wind-generated mixing and entrainment of nutrient-rich hypolimnetic water into the epilimnion. Hydrological income is also small relative to the size of the lake, resulting in a long theoretical hydraulic residence time in the summer of ~ 4.1 years for the year 2007 (Table 3).

The lake stratified intermittently during the summer of 2007 and exhibited periods of hypolimnetic anoxia in the bottom waters of the three basins (Fig. 2). Stratification and the development of hypolimnetic anoxia occurred in mid-June in the deeper north basin and late June in the shallower central and south basins. Mean water-column temperature increased to a peak by early July in the three basins in conjunction with stratification (Fig. 3). An apparent cold front in mid-July resulted in water column cooling and increased susceptibility to mixing and water exchanges. Complete water column mixing

occurred by mid-August in the central and south basins and by early September in the north basin (Fig. 2).

Although Schmidt stability was generally very low for the three basins (relative to deeper lakes), it was greatest in the deeper north basin, which coincided with the development of a longer period of hypolimnetic anoxia that occurred between mid-June and mid-August (Fig. 2). Anoxia extended to the 5-m depth by early July in this basin. Passage of cold fronts, heat loss from the lake, and declines in Schmidt stability in mid-July were accompanied by mixing and reintroduction of dissolved oxygen to deeper depths. Although hypolimnion remained anoxic in the north basin during this period, the vertical extent of anoxia declined from the 5-m to the 7-m depth as a result of mixing. In contrast, the shallower central and south basins completely mixed with reoxygenation of bottom waters. Overall, the anoxic factor was greatest for the north basin at ~ 31 days, followed by the central basin and south basin at ~ 6 and 1 day, respectively.

Water column mean TP and chlorophyll concentrations increased from a minimum in early May to a peak by mid- to late August both lakewide and in each basin (Fig. 4). Maxima in TP and chlorophyll during August were very high in concentration, exceeding 0.10 mg/L and 80 $\mu\text{g/L}$, respectively. Mean summer TP concentrations ranged between 0.083 and 0.092 mg/L while mean summer chlorophyll was 42 to 48 $\mu\text{g/L}$ (Table 4). These ranges translated into a TSI (Carlson Trophic State Index; Carlson 1977) of ~ 68, indicating hypereutrophic conditions.

The time period used for estimating summer $P_{\text{net internal loading}}$ (i.e., equation 3) was based on the net increase in $P_{\text{lake storage}}$ between the late April minimum and the maximum P mass that occurred in September (Fig. 4). $P_{\text{lake storage}}$ mass exhibited a net increase of ~ 3400 kg during this period (Table 5). $P_{\text{external load}}$ was very low, indicating that $P_{\text{net internal load}}$ (solved by difference using equation 3) was the overwhelmingly dominant P source to the lake (Table 5). The area-based $P_{\text{net internal load}}$ (i.e., weighted with respect to lake surface area) was relatively high 2.3 $\text{mg/m}^2 \text{d}$. This rate compared well with an independently-

estimated rate of internal P loading that was based on laboratory-derived sediment fluxes and the occurrence of bottom water anoxia (Table 6; Short Hendrickson Elliott 2009).

Empirical models used in the *Bathtub* projections of mean summer limnological conditions are shown in Table 7. These are commonly used equations for predicting mean summer TP, chlorophyll, and Secchi transparency and based on statistical ranges from numerous lakes in North America. To initialize the model, the lake was segmented into the three basins (Fig. 5) and internal P loading was proportioned according to Table 8, based on calculations reported in Short Hendrickson Elliott (2009). Overall, the north basin represented the greatest internal P loading contribution in conjunction with the highest anoxic factor and a longer period of stratification and bottom water anoxia. By contrast, the central and south basin internal P loading contributions were much lower, coinciding more intermittent stratification, lower anoxic factor values, and much shorter periods of bottom water anoxia. Water mixing and exchange between the north, central, and south basin compartments was also assumed to occur during the summer and thus included in the model setup. This assumption was very realistic given the long fetch parallel to southwest wind rose, the low Osgood Index, and large volume to surface area of the lake. Indeed, summer mean concentrations were similar in each basin, supporting the contention that mixing and horizontal water exchange occur in the lake.

P loading reduction scenarios were as follows,

1. reduce tributary P inputs in 20% increments from 2007 conditions while maintaining internal P loading and
2. reduce tributary P inputs in 20% increments from 2007 conditions and simulate an AI treatment of the north basin by reducing internal P loading to near zero.

Bathtub output closely predicted mean summer TP concentrations both lakewide and for each basin (Fig. 6). Although mean chlorophyll was slightly overpredicted, values were not statistically different than observed means. Predicted Secchi disk transparency was ~ 0.6 m for each basin and lakewide.

Model output suggested that internal P loading, primarily from the north basin, was driving high TP and chlorophyll concentrations in the lake. This predicted outcome was not surprising in light of the high rate of internal P loading determined via budgetary analysis and independent sediment core incubations. Simulated reduction in internal P loading in the north basin resulted in a predicted reduction in mean summer TP of ~ 47% to 0.045 mg/L (Fig. 7 and Table 9). Model output also suggested relatively uniform reductions in TP concentration throughout the lake with internal P loading control in the north basin as a result of horizontal mixing and water exchange between compartments. Internal P loading reduction in the north basin also resulted in a predicted decline in mean summer chlorophyll of ~60% to 21 µg/L and an increase in Secchi transparency to near 1 m (Fig. 7). In contrast, lake variable responses to simulated reductions in tributary P loading were very minor primarily because internal P loading was the dominant P to the lake during the summer (Fig. 8).

Predicted bloom frequency (i.e., percentage of time in the summer that chlorophyll concentration exceeds a given value) would also improve with reduction in internal P loading in the north basin (Fig. 9). For instance, algal blooms exceeding ~ 30 µg/L (i.e., a level at which lake users begin to notice a visible nuisance problem) currently occur about 73% of the time during the summer. Control of internal P loading in the north basin would result in a predicted frequency of occurrence of only ~ 18% of the time (Table 10).

Sediment vertical and spatial characteristics

Moisture content was very high, exceeding 95%, in the upper 3-cm layer of the core collected in the deepest region of the north basin (i.e., station 1; Fig. 10), indicating very flocculent sediment. Organic matter content was also high, representing nearly 40% of the dry mass. Declines in values for moisture and organic matter content with increasing sediment depth were due, in large part, to sediment compaction over time and decomposition of organic matter. Baseline refractory organic matter concentrations occurred below the 15-cm sediment depth at ~ 27%.

Vertical sediment profiles indicated peak concentrations of various P fractions in the upper 10- to 12.5-cm layer. In particular, TP concentrations were extraordinarily high in the upper 5-cm sediment layer, exceeding 4.0 mg/g at the sediment surface. Loosely-bound, iron-bound, and redox-P were also very high in this layer, with iron-bound P accounting for up to 65% of the biologically-labile P (i.e., the sum of redox-P and labile organic P). Concentrations of these constituents declined and were relatively constant below the 15-cm sediment layer. This pattern suggested the buildup of mobile P in the upper sediment layer in excess of breakdown and burial (i.e., *excess* mobile P), a pattern that is typical for eutrophic lake sediments (Carey and Rydin 2011). In particular, peak concentrations of redox-P of ~ 2.5 mg/g near the sediment-water interface were very high and entirely explain the high internal P loading rate in the lake. Mobilization of this P as an internal P load was estimated at 3,591 kg/y, which closely corresponded with other estimates of internal P loading (i.e., Table 6). Overall, vertical profile patterns for redox-P suggested that the upper 10-cm sediment layer at a minimum needed to be considered in aluminum sulfate dosage estimation to control internal P loading in the north basin of the lake (see *Aluminum sulfate dosage determination* below).

Spatially in the north basin, concentrations of loosely-bound and iron-bound P in the upper 5-m sediment layer were greatest at station 1 and declined as a function of decreasing lake depth (Fig. 12 and 13). In contrast, labile organic P was relatively constant at all stations (Fig. 12). Iron-bound P accounted for greater than 50% of the biologically-labile P at stations 1 and 2 (Table 11). Although iron-bound P concentrations were still relatively high at the shallower stations 3 and 4, labile organic P was higher and accounted for > 60% of the biologically labile P.

Aluminum sulfate dosage determination

An example of Rydin and Welch (1999) Al dosage assay results for sediment collected at station 1 is shown in Figure 14. In general, redox-P declined exponentially as a function of increasing Al concentration due to binding onto the Al(OH)₃ floc. The measured Al:P ratio (i.e., parts of Al required to bind one part of redox-P) required to

bind 90% of the redox-P for analyses performed on three different sediment samples was ~ 20:1 (range = 17:1 to 20:1) and fell within regression relationships developed from several lakes in the region (Fig. 15).

To calculate Al dosage for the north basin, an Al:P ratio was estimated for stations 2 to 4 from regression relationships developed between redox-P and the Al:P ratio (Fig. 15). A ratio of 20:1 was used for station 1. The thickness of the sediment layer to be inactivated was set at 10 cm based on *excess* redox-sensitive P observed in the vertical profile at station 1. The Al dosage ranged between 132 and 144 g/m² (mean = 133 g/m²; Table 12).

The Al dosage and cost scenario are shown in Table 13. An Al dosage of 135 g/m² was chosen for treatment. This concentration was slightly higher than the mean (Table 12) to account for any variation in sediment P within the treatment region. Sediment areas located at depths < 20 ft and an additional sediment area encompassing depths < 15 ft (Fig. 16) were chosen for treatment. These areas in the north basin were chosen because they were exposed to anoxia and, thus, had a high potential for anaerobic P release from sediments. Total cost, including a generic setup fee was ~1.72 million dollars (Table 13).

Recent lake Al treatments that have resulted in very effective and successful control of sediment internal P loading and improved water quality have generally ranged between ~ 95 g Al/m² and ~140 g Al/m² (Table 14). These more recent Al dosage ranges are generally higher compared to historical ranges (Huser 2012) because they were targeted toward inactivation of the excess P pool in the sediment. The proposed Al dosage for the north basin of Big Chetac Lake fell within these recent ranges.

Al dosage estimation for the north basin accounted for binding of the more rapidly mobilized redox-P and did not include gradually released labile organic P and slower P diffusion upward from deeper sediments or downward from sediment freshly deposited on top of the Al floc. There is currently some uncertainty regarding whether simply

increasing Al dosage to account for these future P sources will result in the desired longer-term control. de Vicente et al. (2008) showed that aging of the $\text{Al}(\text{OH})_3$ floc without previously sorbed PO_4^{3-} could result in substantially reduced future binding efficiency (up to 75% reduction in adsorption capacity over 90 d) due to changes in crystalline structure of the floc (Berkowitz et al. 2005). They suggested that smaller doses spread out over several years, versus one large dose, might maintain higher binding efficiencies for these future P sources. For the north basin, Al dosage could be adjusted to account for these potential additional sources of P, but more research is needed to clarify both dosage estimation and application strategies for longer-term control of labile organic P and P diffusion from adjacent sediment layers. However, the overall Al dosage proposed for the north basin should be sufficient to bind these future, more gradually released, P sources because the Al dosage is high (Table 14).

The total alkalinity for north basin was moderate at ~ 85 mg CaCO_3/L , suggesting moderate buffering capacity for regulating pH during alum application. Al binding of P is most efficient within a pH range of 6 to 8. As pH declines below 6, Al becomes increasingly soluble (as Al^{3+}) and toxic to biota. The maximum allowable Al dosage for the north basin, determined via jar tests (Cooke et al. 2005), was moderate at 10 mg Al/L (Table 15). Cooke et al. (2005) reported that treatment longevity (i.e., years of successful P control) generally coincided with Al dosages greater than ~ 12 to 18 g/m^3 for stratified lakes (range = 11.7 to 30 g/m^3 ; Table 15). The overall estimated volume-based Al dosage of 19.5 mg/L for the north basin fell well within that reported finding. However, treatment with the proposed areal Al dosage of 135 g/m^2 exceeds the maximum allowable dosage based on a jar test and the nomograph presented in Cooke et al. (2005; page 184). Thus, there would be potential concerns regarding low pH during application. This concern would be alleviated by splitting the application into at least 2 to 3 years (see below). An additional alkalinity-pH vertical profile would need to be examined during the spring to early summer period to verify and refine the maximum allowable Al dose.

There is currently uncertainty regarding the longevity of P control and no predictive models or empirical relationships between the strength of Al dosage and number of years

of internal P loading control. Although essential for cost-benefit analysis, this lack of predictive information is due to minimal long-term limnological monitoring of lakes treated with Al (monitoring costs are a factor). However, Cooke et al. (2005) reported that lakes receiving volumetric dosages of 18 mg Al/L or more exhibited long-term effective internal P loading control and reduction in water column total P concentration (Table 15). Proposed Al dosage for the North basin of Big Chetac Lake fell above 18 mg Al/L (Table 15). Effective reductions in total P concentrations reported in Cooke et al. (2005) ranged from 5 to 18 y and counting (i.e., long-term control in years may be greater but monitoring was stopped). Furthermore, Welch and Cooke (1999) found that experimental sediment P release rates under anaerobic conditions were lowest for lakes treated with Al doses of 18 mg/L or greater.

Aluminum sulfate treatment schedule considerations

Multiple treatments of lower Al concentrations over a period of years (i.e., 1 year intervals) have been successful (Tiefwareensee, Germany) and have merit as a viable treatment schedule for the north basin. For instance, Al could be applied in May at a dosage of $\sim 68 \text{ g/m}^2$ for a two-year period or at a dosage of $\sim 45 \text{ g/m}^2$ for a three-year period. These treatment scenarios would be equivalent to a single application at 135 g/m^2 , but has several advantages. First, splitting the overall Al dosage into 2 or 3 years would ensure that application does not lower pH temporarily to < 6.0 . Second, costs are spread out over a period of several years and may be easier to finance. Third, since each incremental dosage is low relative to the final target dose, the Al floc has a greater chance of becoming saturated with sediment P immediately after application. Other research has suggested that Al binding efficiency for P declines with time as the Al reacts to form more orderly Al-(OOH) polymer chains (Berkowitz et al. 2005, de Vicente et al. 2008). Sediment redox-P and aluminum-bound P could be monitored after each application for effectiveness in control of sediment P. Subsequent Al applications might ultimately be lower if previously applied alum flocs have efficiently inactivated most of the redox-P in the surface sediment layers, resulting in overall cost savings.

ACKNOWLEDGMENTS

Mr. Alex Smith, Wisconsin Department of Natural Resources, is gratefully acknowledged for planning participation. Dr. Randy Hulke, Director of the University of Wisconsin – Stout, Discovery Center, and Dr. Kitrina Carlson, Director of the Sustainability Sciences Institute, are thanked for logistical support during the study. Mr. Jordan Bauer, Ms. Kirsten Reichmann, and Mr. Ryan Veith are gratefully acknowledged for their participation in field sampling and laboratory analyses.

REFERENCES

- APHA (American Public Health Association). 2005. Standard Methods for the Examination of Water and Wastewater. 21th ed. American Public Health Association, American Water Works Association, Water Environment Federation.
- Berkowitz J, Anderson MA, Graham R. 2005. Laboratory investigation of aluminum solubility and solid-phase properties following alum treatment of lake waters. *Wat Res* 39:3918-3928.
- Boström B. 1984. Potential mobility of phosphorus in different types of lake sediments. *Int Revue Ges Hydrobiol* 69:457-474.
- Carlson RE. 1977. A trophic state index for lakes. *Limnol Oceanogr* 22:361-369.
- Carey CC, Rydin E. 2011. Lake trophic status can be determined by the depth distribution of sediment phosphorus. *Limnol Oceanogr* 56:2051-2063.
- Cooke GD, Welch EB, Peterson SA, Nichols SA. 2005. Restoration and management of lakes and reservoirs. 3rd ed. Boca Raton (FL): CRC Press.

- de Vicente I, Huang P, Andersen FØ, Jensen HS. 2008. Phosphate adsorption by fresh and aged aluminum hydroxide. Consequences for lake restoration. *Environ Sci Technol* 42:6650-6655.
- Dugopolski RA, Rydin E, Brett MT. 2008. Short-term effects of buffered alum treatment on Green Lake sediment phosphorus speciation. *Lake Reserv Manage* 24:181-189.
- Gächter R., Meyer JS, Mares A. 1988. Contribution of bacteria to release and fixation of phosphorus in lake sediments. *Limnol Oceanogr* 33:1542-1558.
- Gächter R, Meyer JS. 1993. The role of microorganisms in mobilization and fixation of phosphorus in sediments. *Hydrobiologia* 253:103-121.
- Håkanson L, Jansson M. 2002. Principles of lake sedimentology. The Blackburn Press, Caldwell, NJ USA.
- Hjieltjes AH, Lijklema L. 1980. Fractionation of inorganic phosphorus in calcareous sediments. *J Environ Qual* 8: 130-132.
- Hoyman T. 2012. East Alaska Lake, Wisconsin. *LakeLine* 32(4):34-41.
- Huser B. 2012. Variability in phosphorus binding by aluminum in alum treated lakes explained by lake morphology and aluminum dose. *Wat Res* 46:4697-4704.
- Hupfer M, Gächter R., Giovanoli R. 1995. Transformation of phosphorus species in settling seston and during early sediment diagenesis. *Aquat Sci* 57:305-324.
- Idso SB. 1973. On the concept of lake stability. *Limnol Oceanogr* 18:681-683.
- James WF. 2011. Variations in the aluminum:phosphorus binding ratio and alum dosage considerations for Half Moon Lake, Wisconsin. *Lake Reserv Manage* 27:128-137.
- Jensen HS, Kristensen P, Jeppesen E, Skytthe A. 1992. Iron:phosphorus ratio in surface sediment as an indicator of phosphate release from aerobic sediments in shallow lakes. *Hydrobiologia* 235/236:731-743.
- Lewandowski J, Schauser I, Hupfer M. 2003. Long term effects of phosphorus precipitations with alum in hypereutrophic Lake Süsser See (Germany). *Wat Res* 37:3194-3204.
- Mortimer CH. 1971. Chemical exchanges between sediments and water in the Great Lakes – Speculations on probable regulatory mechanisms. *Limnol Oceanogr* 16:387-404.

Nürnberg GK. 1988. Prediction of phosphorus release rates from total and reductant-soluble phosphorus in anoxic lake sediments. *Can J Fish Aquat Sci* 45:453-462.

Nürnberg GK. 1995. Quantifying anoxia in lakes. *Limnol Oceanogr* 40:1100-1111.

Psenner R, Puckso R. 1988. Phosphorus fractionation: Advantages and limits of the method for the study of sediment P origins and interactions. *Arch Hydrobiol Biel Erg Limnol* 30:43-59.

Rydin E, Welch EB. 1999. Dosing alum to Wisconsin lake sediments based on in vitro formation of aluminum bound phosphate. *Lake Reserv Manage* 15:324-331.

Short Elliott Hendrickson. 2009. Nutrient budget and management data analysis report. Getting rid of the green – phase three. SEH Document No A-BIGCC0701.01. April 2009. Prepared by Short Elliott Hendrickson Inc, Rice Lake WI, for the Big Chetac Chain of Lakes Association.

Wauer G, Gonsioreczyk T, Hupfer M, Koschel R. 2009. Phosphorus balance of Lake Tiefwareensee during and after restoration by hypolimnetic treatment with aluminum and calcium salts. *Lake Reserv Manage* 25:377-388.

Welch EB, Cooke GD. 1999. Effectiveness and longevity of phosphorus inactivation with alum. *Lake Reserv Manage* 15:5-27.

Table 1. Sediment physical-textural characteristics and phosphorus species.	
Category	Variable
Physical-textural	Moisture content
	Wet and dry sediment bulk density
	organic matter content
Phosphorus species	Loosely-bound P
	Iron-bound P
	Labile organic P
	Aluminum-bound P
	Calcium-bound P
	Refractory organic P
	Total P

Table 2. Morphometric characteristics (from Wisconsin Department of Natural Resources).

Characteristic	Value			
Surface area	7,769,971	m ²	1920	ac
Volume	33,438,459	m ³	27109	ac-ft
Mean depth	4.3	m	14.1	ft
Maximum depth	8.5	m	28	ft
Maximum fetch	7.9	km	4.9	mi
Osgood index	1.5			

Table 3. Mean summer (2007) hydrological characteristics (from Short Elliott Hendrickson 2009).

Variable	Value
precipitation over the lake surface (m ³)	3,367,734
inflow (m ³)	5,689,864
lake discharge (m ³)	4,080,285
evaporation (m ³)	5,249,703
Theoretical residence time (y)	4.1
Flushing rate (y ⁻¹)	0.24

Table 4. Mean (MAY-SEP) total phosphorus (P), chlorophyll, and Trophic State Index (TSI; Carlson 1977) for various basins.				
Variable	Lake	North	Central	South
Total P (mg/L)	0.085	0.084	0.083	0.092
Chlorophyll (ug/L)	46	48	42	46
TSI-TP	68	68	68	69
TSI-CHL	68	69	67	68

Table 5. Phosphorus (P) mass balance used to estimate summer net internal P loading in Big Chetak Lake. Please see equation 4 in Methods for term definitions.		
P Flux	4/25/07 - 10/1/07 (159 Days)	
	(kg)	(mg/m ² d)
P _{lake storage}	3365	2.2
P _{external load}	331	0.2
P _{outflow}	502	0.3
P _{net retention}	-171	-0.1
P _{net internal load}	-3536	-2.3

Table 6. Various estimates of internal phosphorus (P) loading for Big Chetac Lake.

Estimate	Internal P load estimate	kg/y	mg/m ² d
1	Net internal P loading from summer P budget (Table 5)	3536	2.3
2	Internal P loading from P release rates ¹	3616	2.3
	Mean internal P load	3576	2.3

¹Short Elliott Hendrickson (2009)

Table 7. Algorithms used for *Bathtub* (Walker 1996) phosphorus loading reduction modeling.

Variable	Model
Phosphorus	Canfield & Bachmann
Chlorophyll	Jones and Bachmann
Secchi Transparency	versus Chlorophyll & Turbidity
Water exchange between segments	Fisher numeric

Table 8. Estimated internal phosphorus (P) load for each basin and percent contribution to the lakewide rate.

Basin	Internal P load		Contribution
	(kg/summer)	(mg/m ² d)	(%)
Chetac Lake	3,616 ¹	2.4	100 ²
North	2,864	5.2	79
Central	500	0.9	14
South	252	0.6	7

¹Short Elliott Hendrickson (2009)

²For instance, internal P loading in the North basin represented 79% of the total internal P load or 2,864 kg/3,616 kg

Table 9. Predicted lake response to tributary phosphorus (P) loading reduction from 2007 conditions and control of internal P loading in the north basin of Big Chetac Lake.

No internal phosphorus loading control						
Tributary P load reduction (% of 2007 conditions)	Predicted Lake Total Phosphorus		Predicted Lake Chlorophyll		Predicted Lake Secchi Transparency	
	(mg/L)	(% reduction)	(ug/L)	(% reduction)	(m)	(% increase)
100	0.085	0	53.2	0	0.51	0
90	0.085	0.4	52.9	0.6	0.52	0.8
80	0.084	0.8	52.6	1.2	0.52	1.6
70	0.084	1.2	52.2	1.8	0.53	2.4
60	0.084	1.6	51.9	2.4	0.53	3.3
50	0.083	2.0	51.6	2.9	0.54	4.1
40	0.083	2.4	51.3	3.5	0.54	5.0
30	0.083	2.9	51.0	4.1	0.55	5.9
20	0.082	3.3	50.7	4.7	0.55	6.8
Internal phosphorus loading control						
Tributary P load reduction (% of 2007 conditions)	Predicted Lake Total Phosphorus		Predicted Lake Chlorophyll		Predicted Lake Secchi Transparency	
	(mg/L)	(% reduction)	(ug/L)	(% reduction)	(m)	(% increase)
100	0.045	47.0	21.0	60.4	0.85	66.0
90	0.044	47.8	20.6	61.3	0.87	69.1
80	0.044	48.6	20.1	62.2	0.89	72.4
70	0.043	49.5	19.6	63.1	0.91	75.9
60	0.042	50.3	19.2	64.0	0.92	79.6
50	0.042	51.2	18.7	64.9	0.94	83.4
40	0.041	52.0	18.2	65.8	0.97	87.6
30	0.04	52.9	17.7	66.7	0.99	92.0
20	0.039	53.8	17.2	67.6	1.01	96.7

Table 10. Predicted bloom frequency to reduction in tributary phosphorus (P) loading from 2007 conditions and control of internal P loading in the north basin of Big Chetac Lake. Red values denote example bloom frequencies as discussed in the Results and Discussion section.

No internal phosphorus loading control						
Tributary P load reduction (% of 2007 conditions)	Predicted frequency that the below chlorophyll concentration is exceeded during the summer growing season (%)					
	> 10 ug/L	> 20 ug/L	> 30 ug/L	> 40 ug/L	> 50 ug/L	> 60 ug/L
100	99.1	89.7	73.0	55.9	41.6	30.7
90	99.1	89.6	72.7	55.6	41.3	30.4
80	99.1	89.4	72.4	55.2	40.9	30.0
70	99.1	89.2	72.0	54.8	40.5	29.7
60	99.0	89.0	71.7	54.4	40.2	29.4
50	99.0	88.8	71.4	54.0	39.8	29.0
40	99.0	88.7	71.0	53.6	39.4	28.7
30	99.0	88.5	70.7	53.2	39.0	28.3
20	98.9	88.3	70.4	52.8	38.6	28.0
10	98.9	88.1	70.0	52.4	38.2	27.7
Internal phosphorus loading control						
Tributary P load reduction (% of 2007 conditions)	Predicted frequency that the below chlorophyll concentration is exceeded during the summer growing season (%)					
	> 10 ug/L	> 20 ug/L	> 30 ug/L	> 40 ug/L	> 50 ug/L	> 60 ug/L
100	81.3	41.0	18.9	8.9	4.4	2.3
90	80.3	39.6	17.9	8.3	4.1	2.1
80	79.3	38.2	17.0	7.8	3.8	1.9
70	78.2	36.7	16.0	7.3	3.5	1.7
60	77.0	35.2	15.1	6.7	3.2	1.6
50	75.8	33.7	14.2	6.2	2.9	1.4
40	74.4	32.2	13.2	5.7	2.6	1.3
30	73.0	30.7	12.3	5.2	2.4	1.1
20	71.4	29.1	11.4	4.8	2.1	1.0
10	69.8	27.5	10.5	4.3	1.9	0.9

Table 11. Textural and chemical characteristics of the upper 10-cm sediment sections collected at variation stations in Big Chetac Lake.

Station	Depth		Section		Moisture content (%)	Density		Organic matter (%)	Total P (mg/g)	Loosely-bound P (mg/g)	Iron-bound P (mg/g)	Labile organic P (mg/g)
	(m)	(ft)	upper (cm)	lower (cm)		Dry (g/cm ³)	Wet (g/cm ³)					
1	7.8	25.6	0	5	95.6	0.045	1.017	40.0	2.929	0.246	1.170	0.600
			5	10	94.2	0.056	1.022	34.5	1.657	0.086	0.562	0.372
2	6.9	22.6	0	5	95.6	0.045	1.017	28.6	2.359	0.107	0.822	0.619
			5	10	94.2	0.059	1.023	30.9	1.503	0.016	0.170	0.487
3	5.1	16.7	0	5	94.0	0.062	1.024	32.2	1.686	0.017	0.309	0.414
			5	10	92.1	0.083	1.036	32.7	0.959	0.010	0.083	0.252
4	3.5	11.5	0	5	93.9	0.063	1.024	29.8	1.329	0.011	0.166	0.363
			5	10	91.5	0.089	1.037	33.7	1.031	0.009	0.092	0.196

Table 12. The estimated redox-sensitive phosphorus (P) concentration over the upper 10 cm, aluminum:phosphorus (Al:P) binding ratio, estimated thickness of the excess sediment P layer to be treated with aluminum sulfate (as aluminum; Al), and the areal Al dosage estimate for various stations in the north basin of Big Chetac Lake.

Depth contour (ft)	Station	Mean redox-sensitive P ¹	Estimated Al:P ratio	Treated sediment thickness (cm)	Al dose (g/m ²)
>25	1	1.409	20 ²	10	132
20-25	2	0.507	51 ³	10	133
15-20	3	0.193	104	10	144
10-15	4	0.133	137	10	137

¹Represents an integrated mean over the upper 10 cm

²Measured (Figure 14)

³Estimated from regression equation shown in Figure 15

Table 13. Approximate cost scenario to treat the north basin with aluminum sulfate.

Variable	Cost estimate
Acres	462
Al dosage (g/m ²)	135
Alum (\$)	\$1,708,443
Setup (\$)	\$10,000
Total (\$)	\$1,718,443

Table 14. Recent and proposed alum (as Al) dosages for various lakes. An asterisk denotes a future treatment.

Lake	Al Dose (g Al m ⁻²)	Reference
Big Chetac, WI	135	Present study
Successful treatments		
Black Hawk, MN	145	James (unpubl. Data)
Tiefwareensee, Germany	137	Wauer et al. (2009)
East Alaska, WI	132	Hoyman (2012)
Half Moon, WI ¹	115	James (2011)
Susser See, Germany	100	Lewandowski et al. (2003)
Green, WA	94	Dugopolski et al. (2008)
Proposed future treatments		
Squaw, WI*	120	James (unpubl. data)
Cedar, WI ²	116	James (unpubl. data)
Halsted's Bay, Minnetonka, MN ³	105	James (unpubl. data)
Bald Eagle, MN*	100	James (unpubl. data)

¹West and east arm dosages were 150 and 75 g/m², respectively

²Average of a stratified treatment at 130 and 100 g/m²

³Average of a stratified treatment at 140 and 80 g/m²

Table 15. A comparison of the maximum allowable Al dose, based on a titration assay and nomograph estimate presented in (Cooke et al. 2005) and the the areal sediment redox-P based Al dosage converted to a concentration for the north basin. Al dosages and longevity for other unstratified and stratified lakes are from Cooke et al (2005). Numbers on parentheses denote percent reductions in in total phosphorus. Longevity = as of publication of Cooke et al. (2005).

Lake	Al Dose (g Al/m ³)	Observed Longevity (years)
North Basin Big Chetac Lake	Maximum allowable 10.0 to 12.5 Estimated based on Rydin and Welch (1999) 19.5	
Unstratified lakes	Long Kitsap County 5.5 Pickerel 7.3 Long Thurston County North 7.7 Pattison North 7.7 Wapato 7.8 Erie 10.9 Campbell 10.9	11(30%) <1 >8 (56%) 7 (29%) <1 >8 (75%) >8 (46%)
Stratified lakes	Eau Galle 4.5 Morey 11.7 Cochnewagon 18 Dollar 20.9 Annabessacook 25 West Twin 26 Irondoquoit Bay 28.7 Kezar 30	<2 8 (60%) 6 (not reported) 18 (68%) 13 (41%) 18 (66%) 5 (24%) 9 (37%)

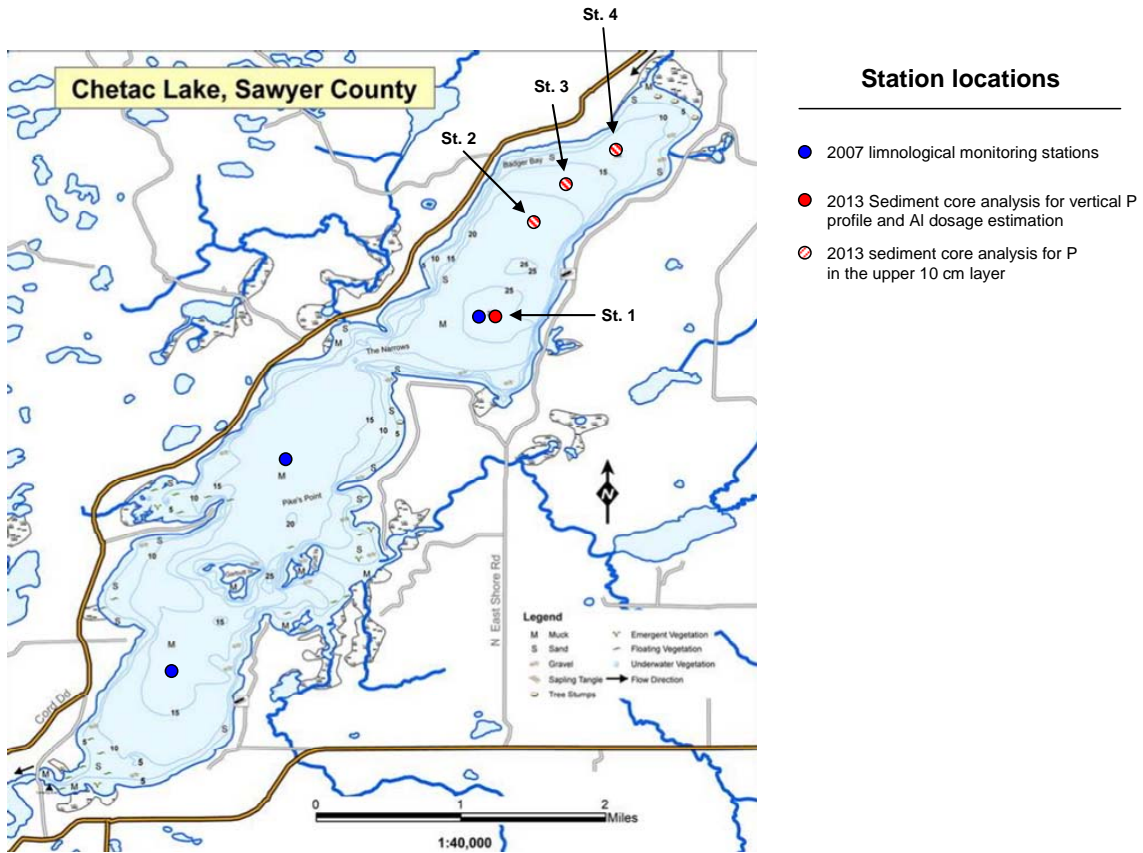


Figure 1. Bathymetric map of Big Chetac Lake with various station locations.

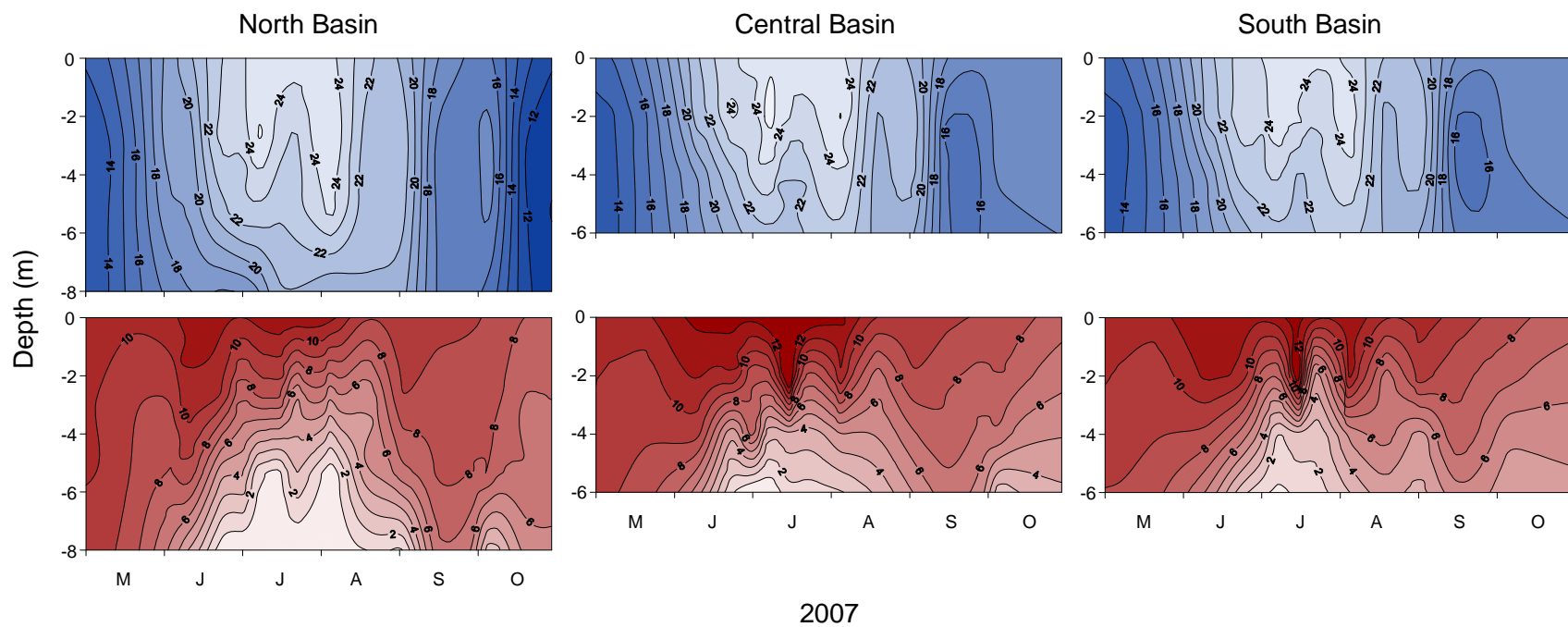


Figure 2. Seasonal and vertical variations in temperature (upper panels) and dissolved oxygen (lower panel) in the north, central, and south basins of Big Chetac Lake in 2007.

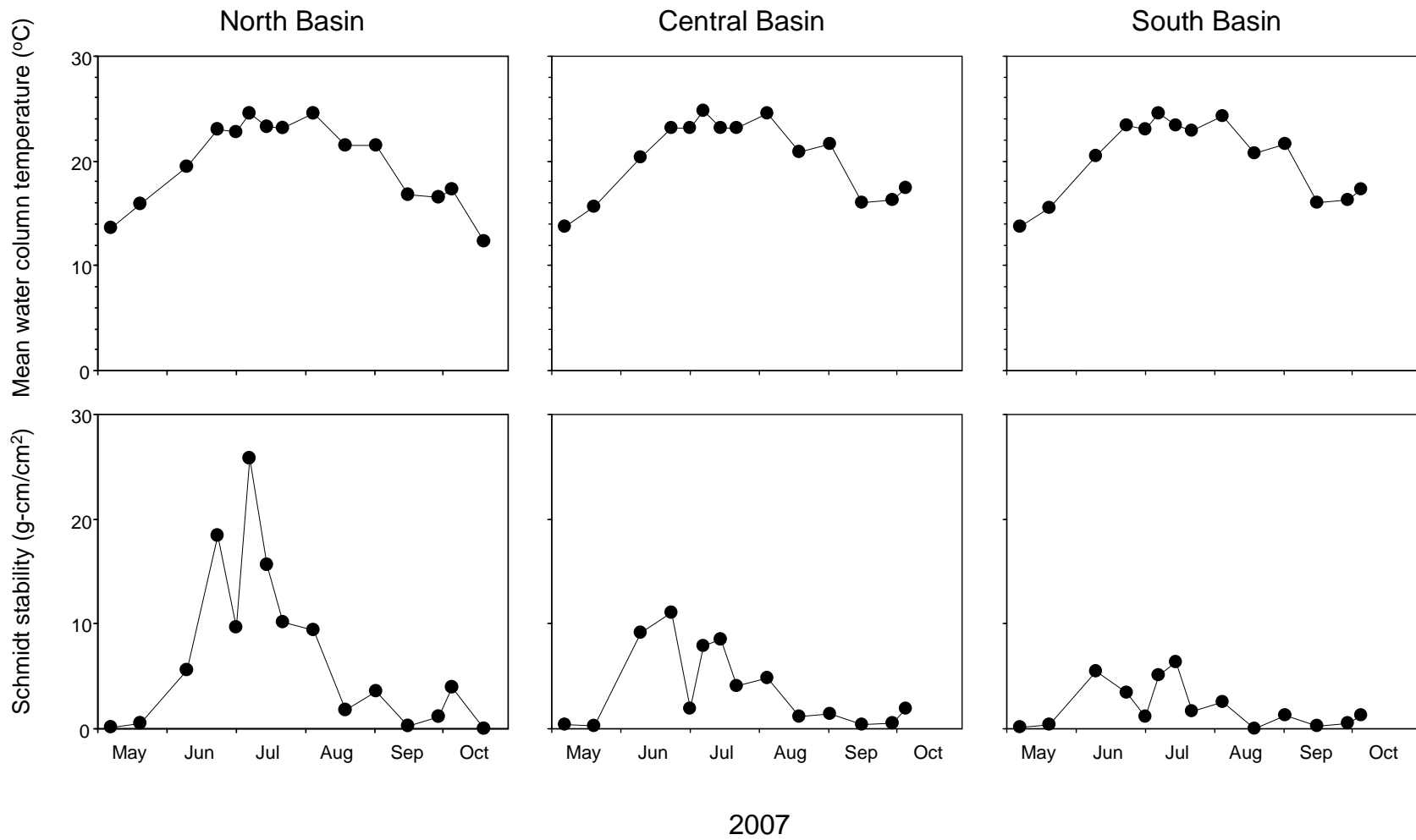


Figure 3. Seasonal variations in mean lake temperature (upper panels) and Schmidt stability (lower panels) in the north, central, and south basins of Big Chetac Lake in 2007.

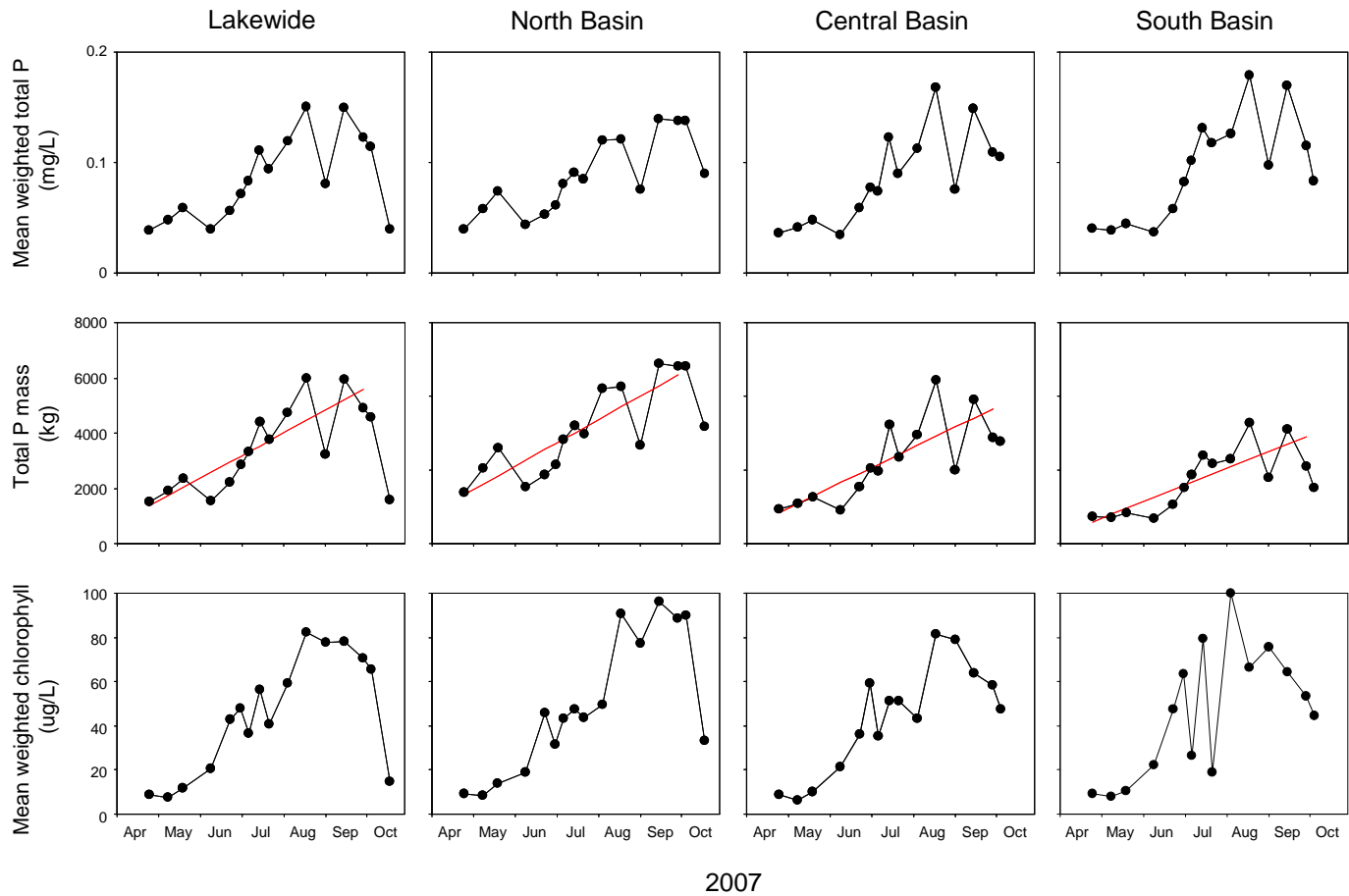


Figure 4. Seasonal variations in mean water column total phosphorus (P) concentration (upper panels), total P mass (middle panels), and mean water column chlorophyll (lower panels) lakewide (i.e., mean for the entire lake) and in the north, central, and south basins of Big Chetac Lake in 2007. Red bar denotes the time period used to estimate net internal phosphorus loading.

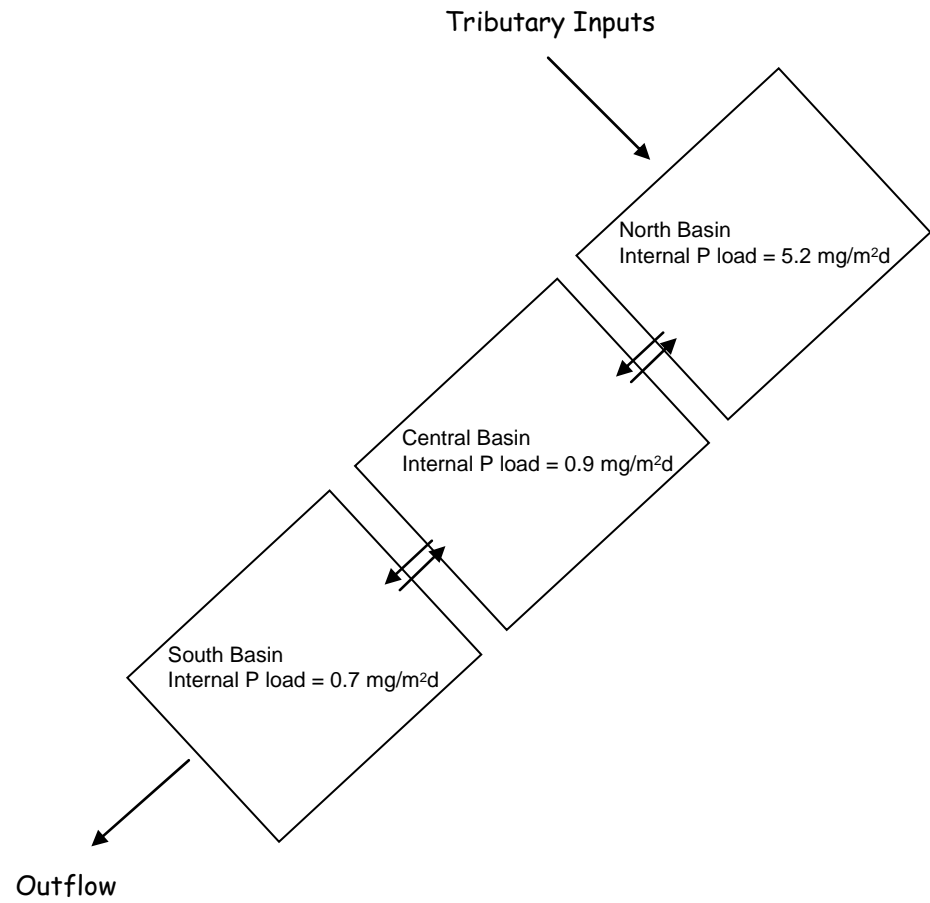


Figure 5. Conceptual diagram of segments used for empirical steady-state modeling.

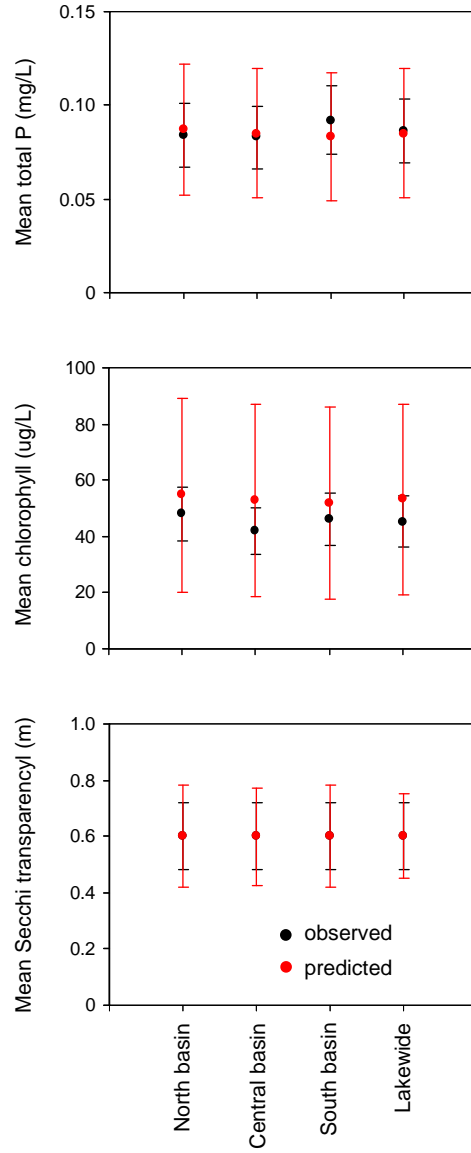


Figure 6. Observed and predicted mean summer concentrations under 2007 tributary and internal phosphorus (P) loading conditions. Vertical bars represent 1 standard deviation.

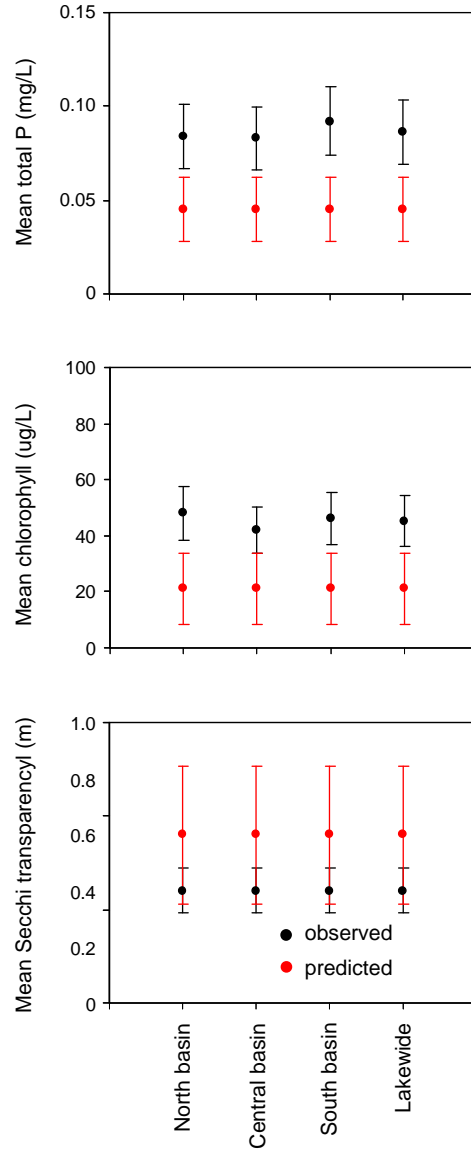


Figure 7. Observed and predicted (Bathub; Walker 1996) mean summer concentrations after simulated internal phosphorus (P) loading reduction in the north basin. Vertical bars represent 1 standard deviation.

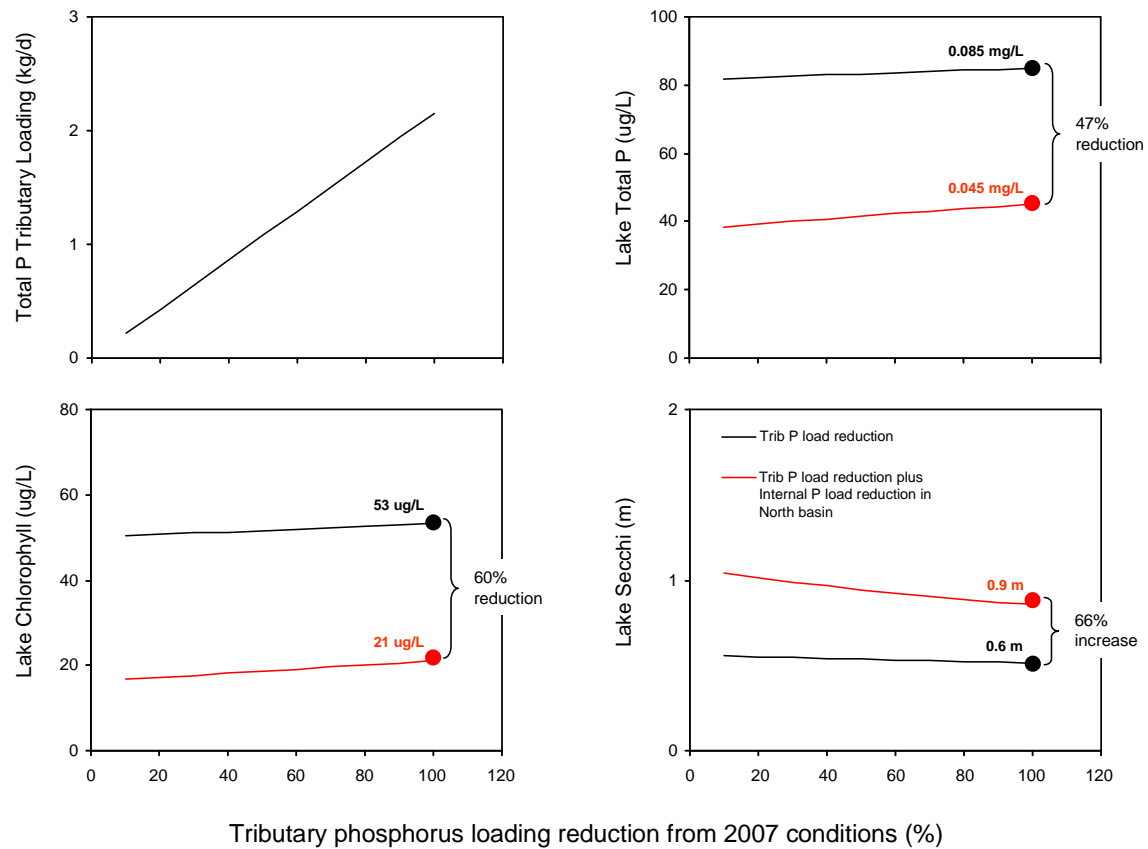


Figure 8. Bathtub (Walker 1996) model output of predicted changes in mean summer lake total phosphorus, chlorophyll, and Secchi transparency as a function of increases or decreases in 2007 tributary P loading conditions (black lines) and tributary plus reduction in internal P loading in the north basin (red lines).

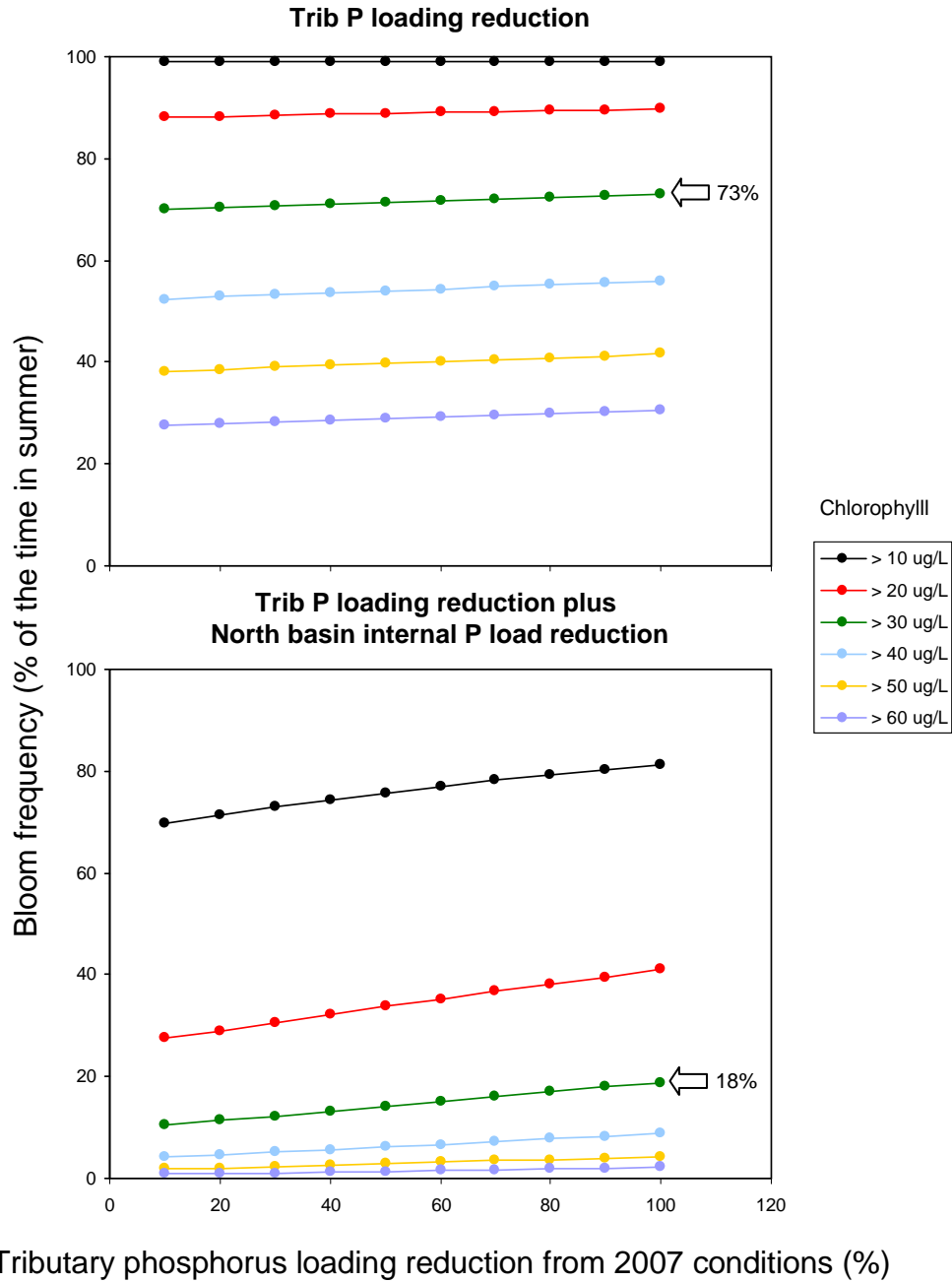


Figure 9. Bathtub (Walker 1996) model output of predicted changes in algal bloom frequency of occurrence (as chlorophyll) as a function decreases in 2007 tributary P loading conditions (upper panel) and tributary plus reduction in internal P loading (lower panel).

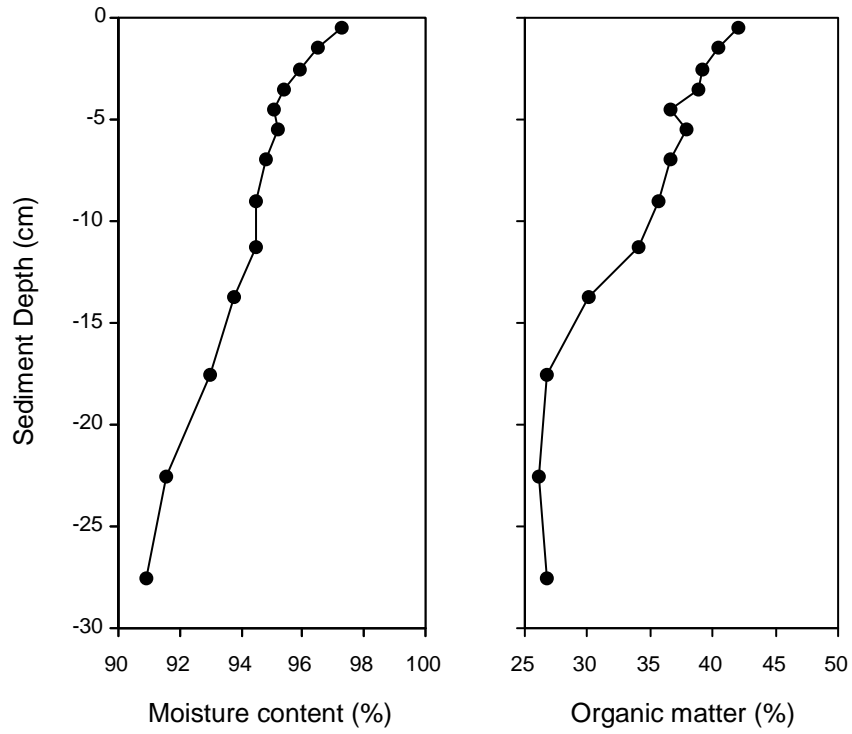
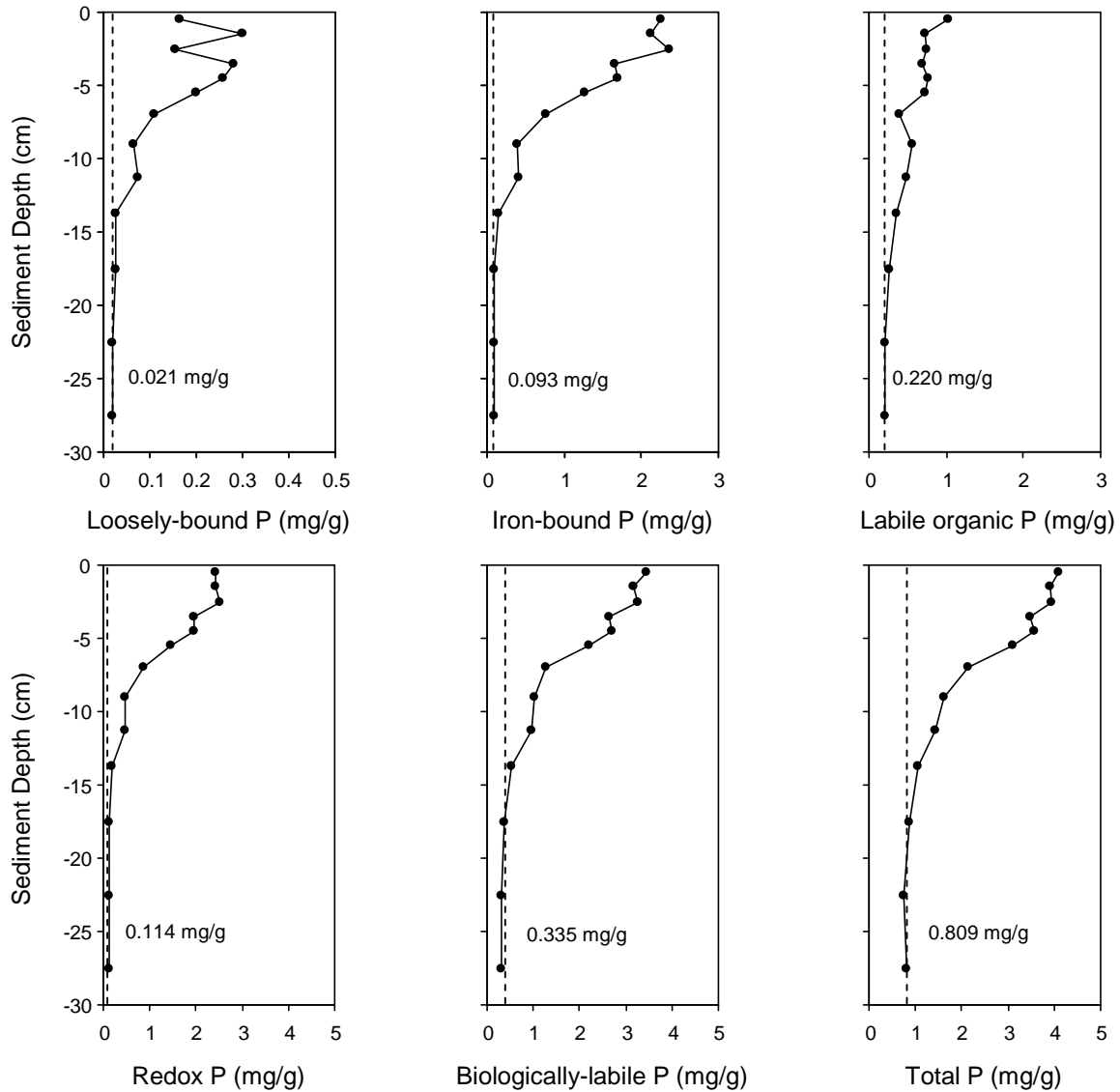


Figure 10. Vertical variations in moisture content and organic matter at station 1 in the north basin of Big Chetac Lake.



Sediment P fraction

Figure 11. Vertical variations in phosphorus (P) fractions at station 1 in the north basin of Big Chetac Lake. Redox-sensitive P represents the sum of the loosely-bound and iron-bound P fractions and is correlated with anaerobic P release rates from sediment. Biologically-labile P, the sum of redox-sensitive P and labile organic P fractions, is generally subject to recycling pathways the result in diffusive P flux to the overlying water column. Dashed lines represent mean background concentrations estimated as the average below the ~ 15-cm depth. The area encompassed by the dashed line and peak concentrations at sediment depths less than 10 cm represents biologically-labile and redox-sensitive P in excess of burial and diagenesis.

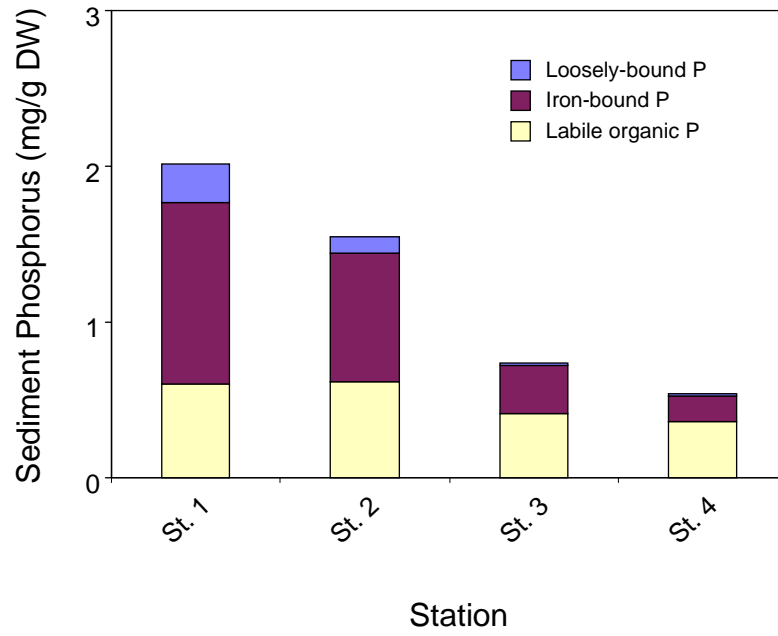


Figure 12. The composition of biologically-labile sediment phosphorus (P) at stations 1 to 4 in the north basin of Big Chetac Lake.

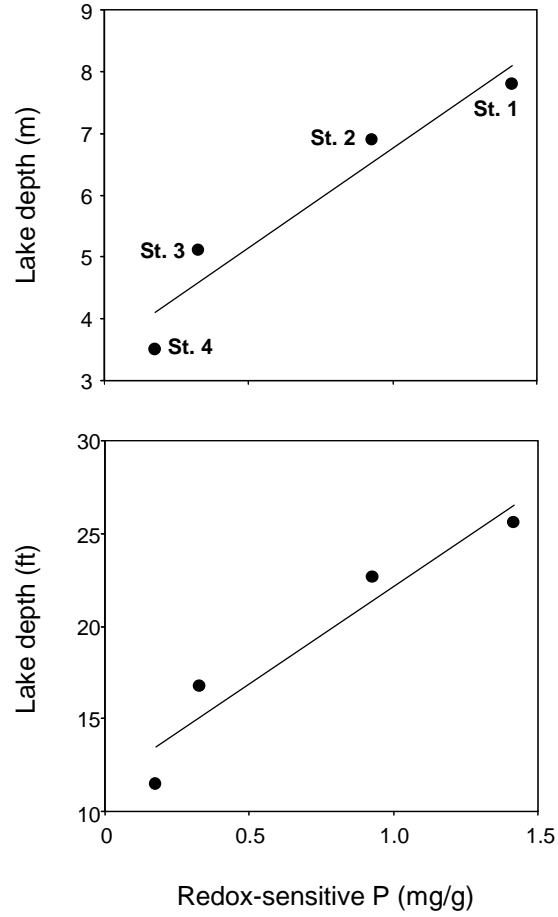


Figure 13. Relationships between redox-sensitive phosphorus (P) concentrations in the sediment and lake depth.

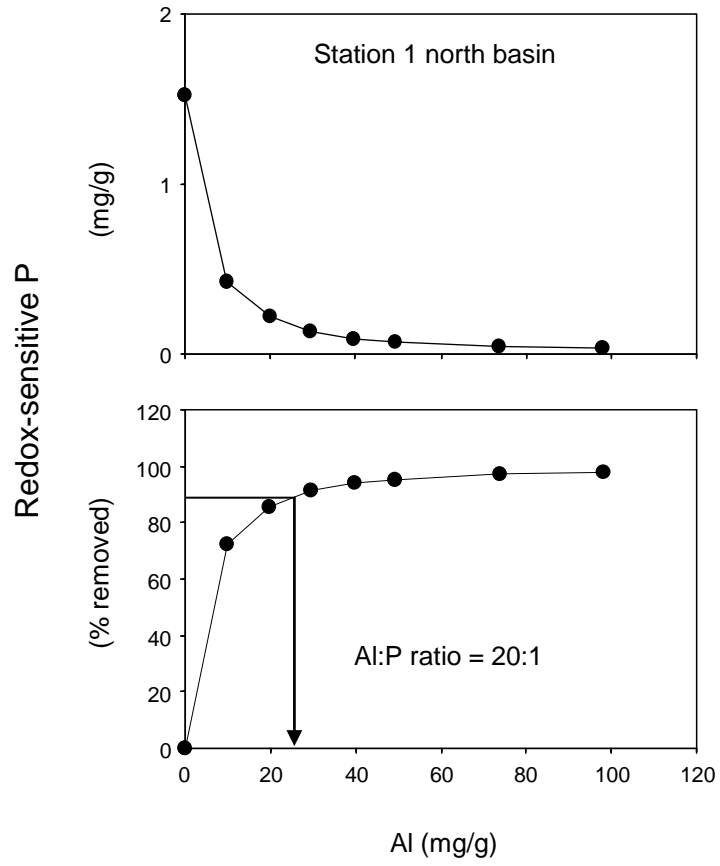


Figure 14. Variations in the concentration of redox-sensitive phosphorus (P; upper panel) and percent removed or adsorbed to the aluminum (Al) floc (lower panel) as a function of increasing Al concentration.

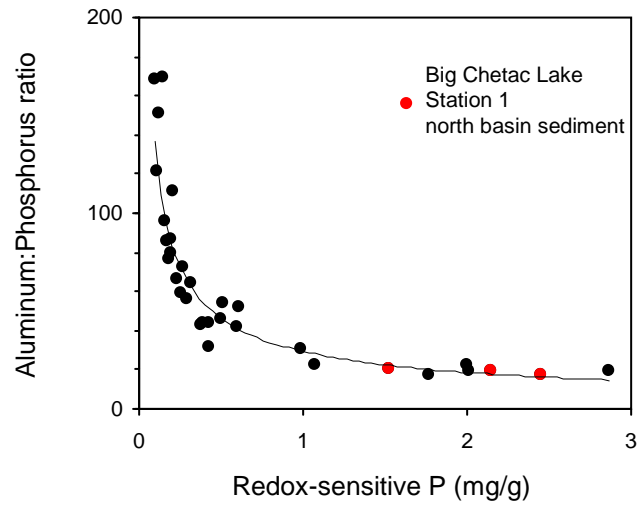


Figure 15. Relationships between the redox-sensitive phosphorus (i.e., the sum of the loosely-bound and iron-bound phosphorus, P) concentration and the Al:P ratio (i.e., the mass of Al required to bind at least 90% of the redox-sensitive P). The red circles represent assays for sediment collected in the north basin of Big Chetac Lake.

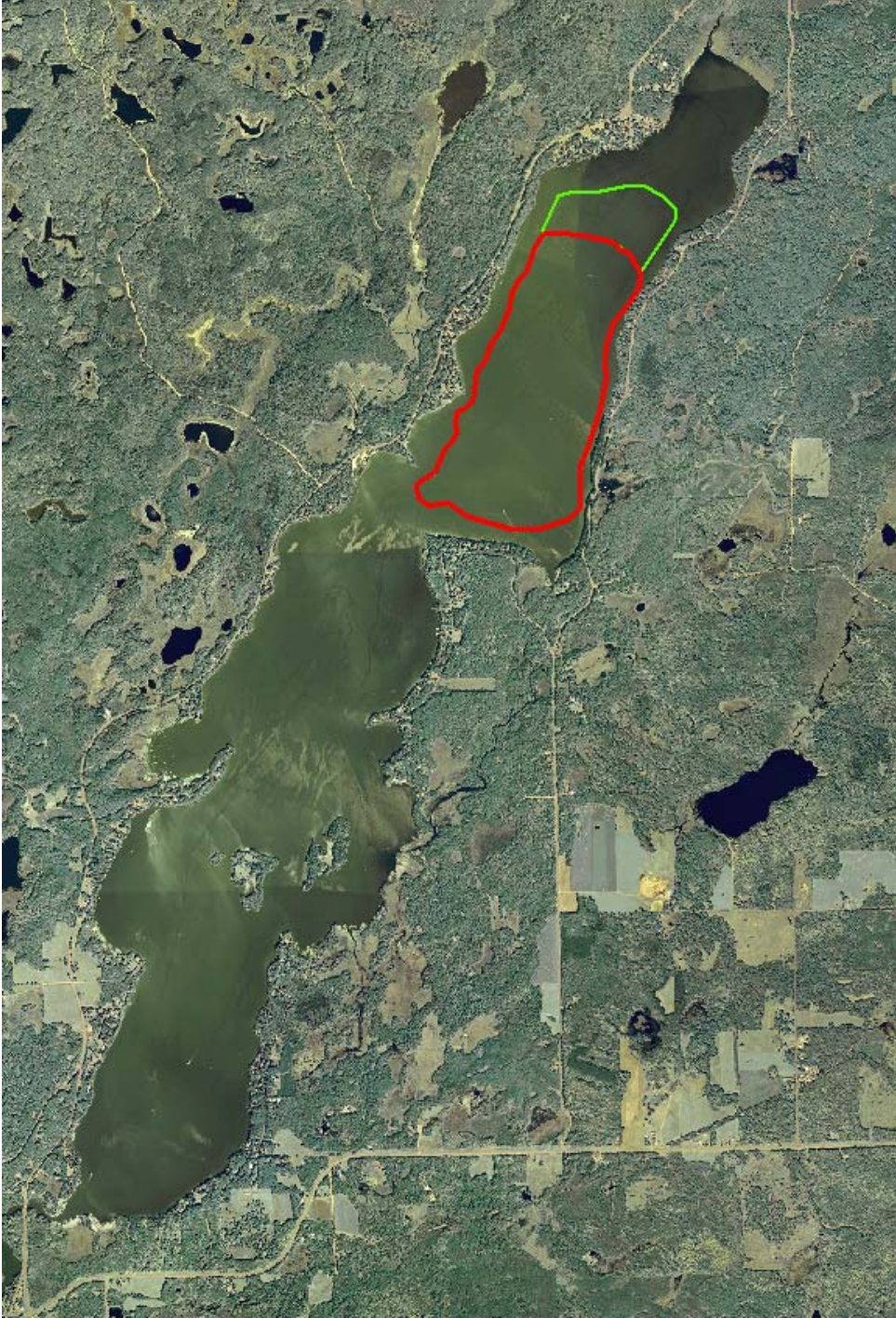


Figure 16. Location of the proposed aluminum sulfate treatment area in the north basin of Big Chetac Lake. The area enclosed by the red line represents sediments below the 20-ft contour while the green line represents a sediment area located north of the deepest region at lake depths greater than 15 ft. The entire area enclosed by these lines is recommended for Al treatment.